

## NUCLEON-NUCLEUS INELASTIC SCATTERING

Charles Glashausser  
Rutgers University  
New Brunswick, NJ 08903  
USA

My task today is to review some recent developments in inelastic scattering at intermediate energy from an experimentalist's point of view, and also to get you out of here in time for lunch. The latter task is clearly more important, but I can certainly accomplish it with your help if I whet your appetite sufficiently. The meat of my talk concerns measurements and interpretations (relativistic and non-relativistic) of spin rotation parameters  $D_{ij}$ . First, however, I want to discuss briefly the energy dependence of cross section  $\sigma$  and analyzing power  $A_y$  results, and then a new sophisticated analysis of  $^{16}\text{O}$  and  $^{18}\text{O}$  data aimed at determining the shapes of neutron transition densities with high precision. After reviewing recent measurements of  $D_{ij}$ , I want to mention finally the current status of our work on spin excitations in nuclei. Much of the data that I shall be reporting on is the work of others and should be considered preliminary; I am grateful to my colleagues for providing this material.

Let me begin with a somewhat old-fashioned topic, a macroscopic coupled-channels analysis of  $^{12}\text{C}$  data,<sup>1</sup> shown in Fig. 1. The calculations, carried out primarily by R. de Swiniarski with the code ECIS, are shown by the solid lines. The fits, particularly for the cross sections, are very good over the entire energy range, much better than fits for  $^{12}\text{C}$  at lower energies. What is particularly interesting however, is that they yield a value for the deformation  $\delta$  ( $=\beta R$ ) which is essentially constant over this range of incident energies, as shown in Table 1; these values agree also with previous determinations at lower energies. Similar results were obtained for other natural parity states in  $^{12}\text{C}$ . Now, insofar as  $\delta_L$  can be thought to be directly related to  $B(\text{EL})$ , the constant value is reassuring; a property of the nucleus seems to be determined and the present result thus seems to reinforce many similar results obtained for a wide range of nuclei at low energies. But life should not be so simple, as Osterfeld et al. have shown:<sup>2</sup> the shape of the effective transition operation for inelastic proton scattering changes with bombarding energy, so there is little reason to expect the close correspondence between  $B(\text{EL})$  and  $\delta_L$  to be maintained over a wide

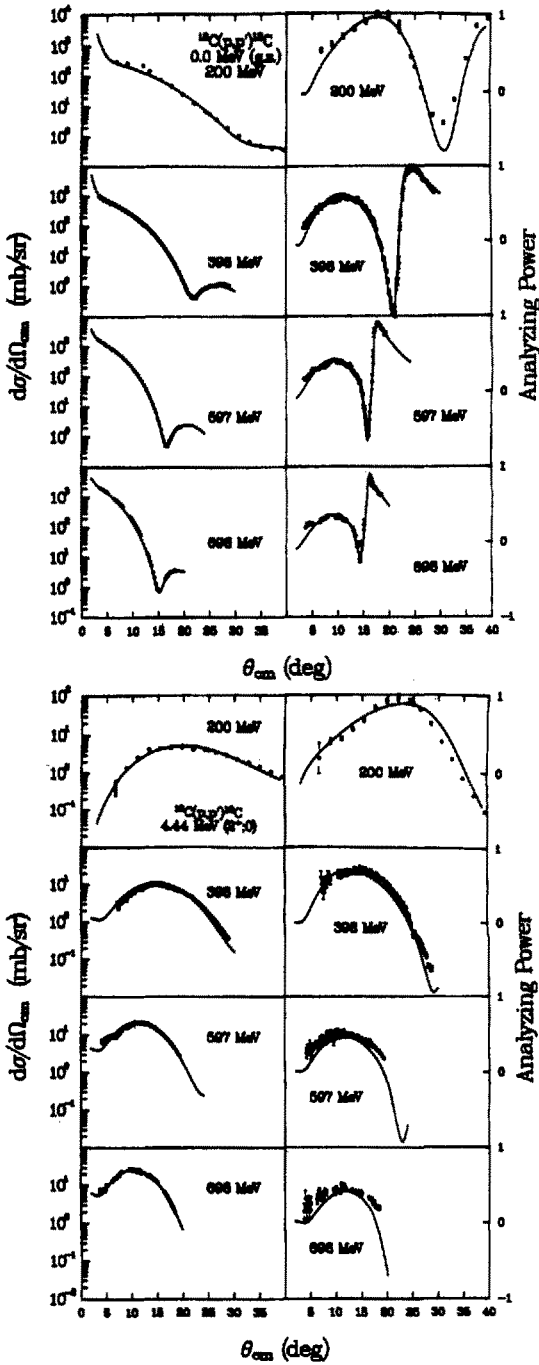


Figure 1. Macroscopic model coupled-channels analysis of data for the ground state (top) and first  $2^+$  state (bottom) in  $^{12}\text{C}$  at incident energies of 200, 398, 597, and 697 MeV (Ref. 1). Differential cross sections are shown on the left; analyzing powers on the right. The higher energy data were binned in very fine steps and appear almost as a continuous line. The data for the first  $4^+$  state were also included in the analysis.

Table 1. Values of deformation parameters  $\delta$  and renormalization factors N determined from the macroscopic and microscopic analysis of the  $^{12}\text{C}(p,p')^{12}\text{C}(2^+)$  reaction at different energies.

$E_p$ (MeV)	$\delta$ (fm)	N
30-40	-1.61	
200	-1.62	1.0
398	-1.68	1.81
597	-1.70	2.09
698	-1.60	2.09
800	-1.70	2.36
1040	-1.73	

energy range. Some previous results, particularly in the 100-200 MeV range,<sup>3</sup> have revealed large discrepancies with low energy values of  $\delta_L$ , although measurements at 800 MeV have generally been consistent with the data at  $E_{\text{inc}} < 100$  MeV. Much of the available data in the 100 to 800 MeV range has not been subjected to a simple macroscopic analysis, since the aim of the experiments was to obtain detailed microscopic information about the transition density. The present results suggest that an effort to understand the present body of intermediate energy data in terms of the simple model might yield interesting results. In the  $^{12}\text{C}$  case, for example, it may be that the expected changes with energy are cancelled by changes in the deformation of the different regions of the nucleus being sampled, as electron scattering results suggested some time ago.<sup>4</sup>

The other side of the coin is that good microscopic wave functions in a reliable theory should be able to explain the data equally well at all energies. Distorted-wave impulse approximation (DWIA) calculations<sup>5</sup> based on Cohen-Kurath wave functions for  $^{12}\text{C}$  and the Love-Franey t-matrix are shown in Fig. 2 for the  $2^+$  state at 4.44 MeV and also for the  $1^+$ , T=0 state at 12.71 MeV. These microscopic predictions for the  $2^+$  state are almost as good as the macroscopic calculations shown above; the curves for the  $1^+$  state also agree reasonably well with the data. The renormalization factors which multiply the theoretical cross sections for the  $2^+$  state are shown in Table 1. In the energy region of 400-700 MeV illustrated in Fig. 2, this renormalization factor is constant at about 2.0, and this factor agrees with the renormalization factor from electron scattering. At 200 MeV, however, the renormalization factor is only 1.0, and this discrepancy has not been explained. There have not been enough systematic microscopic analyses of

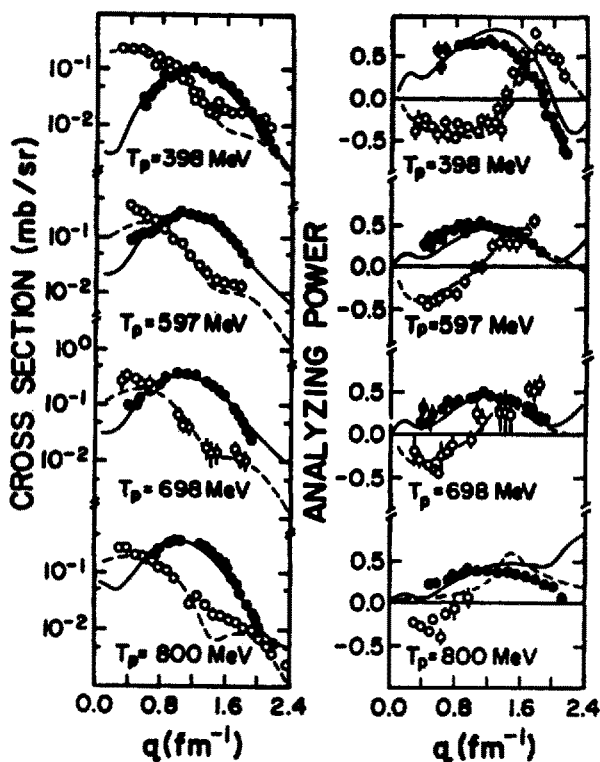


Figure 2. Cross sections and analyzing powers for the 4.44 MeV (solid circles  $\times 0.01$ ) and 12.71 MeV (open circles) states in the  $^{12}\text{C}(p,p')^{12}\text{C}^*$  reaction as a function of incident proton energy. The DWIA calculations are shown as solid and dashed curves for the 4.44 MeV and 12.71 MeV states, respectively (Ref. 5).

natural parity states around 200 MeV to determine if this problem is a general one, due to problems in the reaction theory such as density dependence in the interaction or relativistic effects as we are discussing at this conference, or whether it is a problem in the wave function for the  $2^+$  state in  $^{12}\text{C}$ .

An ambitious effort to determine neutron transition densities  $\rho_n(r)$  from inelastic proton scattering has been undertaken by J. Kelly and co-workers.<sup>6</sup> Certainly this has been a goal of intermediate energy proton scattering for a long time, and at least partial success has been achieved for elastic scattering, in the sense that differences in ground state neutron densities between neighboring

isotones can be determined now with reasonable accuracy. As the discussion of relativistic impulse approximation techniques at this meeting suggests, the reaction theory is not yet good enough to make reliable estimates of the absolute differences between neutron and proton densities for a given nucleus as accurately as the intrinsic sensitivity of proton scattering would suggest is possible. A similar, even more difficult, situation prevails for inelastic scattering, so that no previous attempt has been made to really explore the sensitivity of the inelastic proton probe in the same way that inelastic electron scattering has been examined.

In Kelly's method, an empirical density-dependent nucleon-nucleon interaction at 135 MeV is determined by fitting data for nine states in  $^{16}\text{O}$  of different spins and multipolarities (and thus transition densities which peak at different regions in the nucleus). In this fit, the neutron transition densities in  $^{16}\text{O}$  are assumed equal to the proton transition densities  $\rho_p(r)$  by charge independence and the proton densities are known from electron scattering. The unknown neutron transition density is then expanded as follows:

$$\rho_L(r) = \alpha^3 y^L e^{-y} \sum_{n=0}^{\infty} a_n y^{2n},$$

where  $y = \alpha r$  and  $\alpha$  is the oscillator parameter. The empirically determined interaction is used, and the parameters  $a_n$  are varied until a good fit is obtained to the cross section data. The results for the first  $2^+$  state in  $^{18}\text{O}$  are shown in Fig. 3, where the neutron transition density so obtained is compared with the proton transition density (multiplied by the appropriate normalization factor) determined from electron scattering. The important result, as we shall see, is not the difference between  $\rho_n$  and  $\rho_p$ , but rather the sensitivity band for  $\rho_n$  as shown by the shaded area. If this sensitivity band were really an error band, i.e., if it included the model dependence of the procedure, the result would show that protons are almost as valuable in determining neutron transition densities as electrons are in determining proton transition densities. (Even then, the very narrow band at the center is somewhat misleading, since the fits are constrained to go as  $r^L$  at small  $r$ .)

The results are, however, quite model dependent. Kelly et al. have shown this by using their empirical interaction to precisely fit the cross section data for the first  $2^+$  state in  $^{16}\text{O}$  assuming that  $\rho_n$  is unknown. This state was one of the nine used to

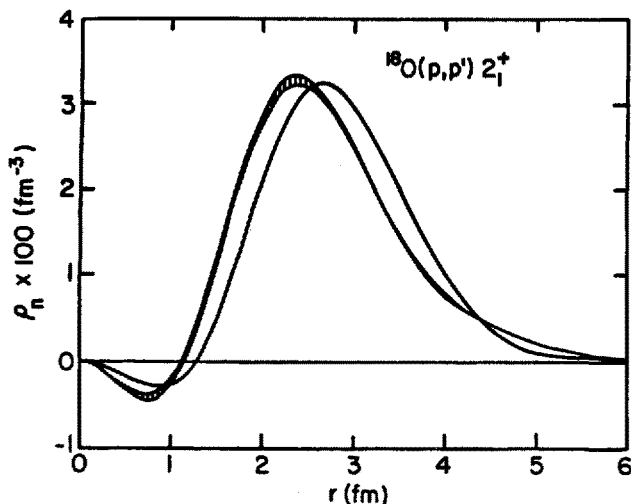


Figure 3. Comparison of the neutron transition density  $\rho_n(r)$  (shaded) deduced from analysis of the  $^{18}\text{O}(p,p')^{18}\text{O}(2^+)$  reaction data at 135 MeV with the proton transition density  $\rho_p(r)$  previously determined from electron scattering (Ref. 6). The shaded area in  $\rho_n(r)$  represents the sensitivity band as explained in the text.

determine the empirical interaction with  $\rho_n$  set equal to  $\rho_p$ ; the fit to the  $2^+$  cross section was good, but some small discrepancies were apparent. The changes in  $\rho_n$  necessary to provide a perfect fit to the  $2^+$  data are a measure of the intrinsic error of the whole procedure. Unfortunately these changes in  $\rho_n$  are substantial, surprisingly large to me given the rather small initial disagreement between "theory" and experiment for this state. The fitted  $\rho_n(r)$  for  $^{16}\text{O}$  is substantially different from the known  $\rho_p(r)$ ; the differences are far outside the sensitivity band. Thus the procedure cannot be trusted to reliably yield small differences between  $\rho_n(r)$  and  $\rho_p(r)$  such as those in Fig. 3 for  $^{18}\text{O}$ . When the derived differences between  $\rho_n(r)$  and  $\rho_p(r)$  are large, however, as they sometimes are in heavier nuclei, then the method can be used to obtain at least a qualitative measure of these differences, as Kelly has shown very recently in  $^{88}\text{Sr}$ , for example.<sup>7</sup>

We turn now to the measurement of the spin rotation parameters  $D_{ij}$  for the inelastic scattering. Primarily because of the importance of the first measurements of  $D_{ij}$  at LAMPF in pointing up the

apparent necessity of a relativistic treatment for elastic scattering, such measurements are becoming very popular. The notation is not yet uniform, but it is common that the first index  $i$  refers to the polarization state of the incident beam and  $j$  to the measured polarization state of the scattered particle. Each index can be 0 (unpolarized),  $n$  (normal to the scattering plane),  $l$  (longitudinal, along the particle direction), and  $s$  (sideways, perpendicular to the particle direction in the scattering plane). A measurement of  $D_{ls}$ , for example, requires an incident beam polarized along the beam direction and a measurement of the sideways component of the polarization of the outgoing particle. This measurement is now universally carried out with a polarimeter in the focal plane of a large spectrometer. The polarimeter is basically a thick carbon target (large enough to intercept particles over most of the focal plane) followed by a series of wire chambers for position identification of particles scattered from the carbon in two directions. A schematic diagram of the LAMPF polarimeter<sup>8</sup> is shown in Fig. 4. Because the  $n$  and  $l$  components of the spin of the scattered

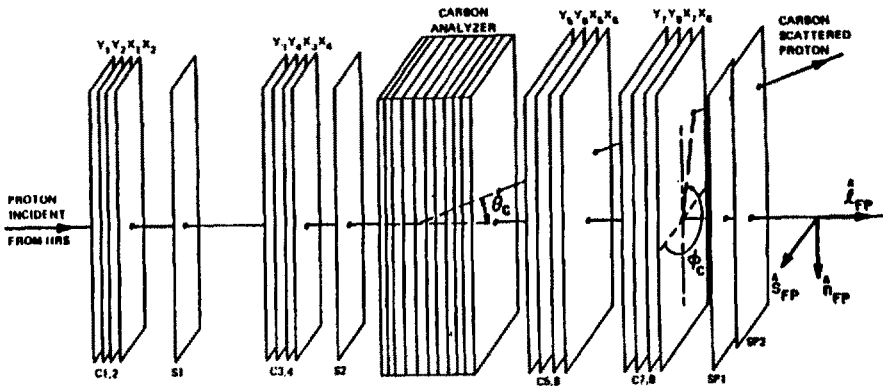


Figure 4. Schematic diagram of the focal plane polarimeter at the High Resolution Spectrometer at LAMPF (Ref. 8). The counters labelled C1-C8 are wire chambers; S1, S2, SP1 and SP2 are scintillators. The carbon analyzer is a set of carbon blocks whose thickness is varied as a function of the energy of the scattered particles.

particle precess in passing through the vertical LAMPF spectrometer, both may be measured at suitable energies where neither is longitudinal at the focal plane.

Some very recent examples of such measurements, for the  $3^-$  state

in  $^{16}\text{O}$  at an incident energy of 498 MeV, are shown in Figs. 5-7.

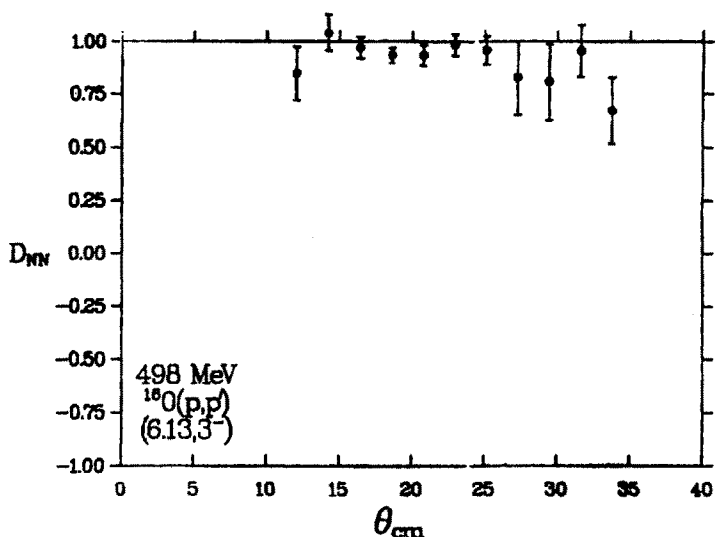


Figure 5. Preliminary values of  $S_{\text{NN}}$  for the  $^{16}\text{O}(p,p')^{16}\text{O}$  ( $3^-, 6.13 \text{ MeV}$ ) reaction at 498 MeV (Ref. 9).

These preliminary data were taken by D. Lopiano et al. at LAMPF.<sup>9</sup> Previous theoretical and experimental work<sup>10</sup> has shown that the  $D_{ij}$  parameters for strong natural parity  $\Delta S=0$  excitations should be expected to follow the same rules which are required by symmetry considerations for elastic scattering:

$$D_{\text{NN}} = 1; D_{\text{LL}} = D_{\text{SS}}; D_{\text{LS}} = D_{\text{SL}}.$$

The data shown do illustrate these rules very nicely. No theoretical calculations have yet been carried out for these data, or for similar data<sup>10</sup> on natural parity states in  $^{40}\text{Ca}$  (except for an interesting relativistic calculation just received and mentioned below).

Theoretical interest in such measurements has centered mainly on  $\Delta S=1$  transitions to unnatural parity states. Such data<sup>11</sup> at 500 MeV for the 12.71 MeV,  $1^+$ ,  $T=0$  state and the 15.11 MeV,  $1^+$ ,  $T=1$  state in  $^{12}\text{C}$  are shown in Fig. 8. The data shown are labelled  $D_{\text{O}}$ ,  $D_{\text{X}}$ ,  $D_{\text{Y}}$ , and  $D_{\text{Z}}$ ; these parameters are linear combinations of the  $D_{ij}$  parameters which, in the plane wave impulse approximation, have been shown to be uniquely sensitive to individual terms in

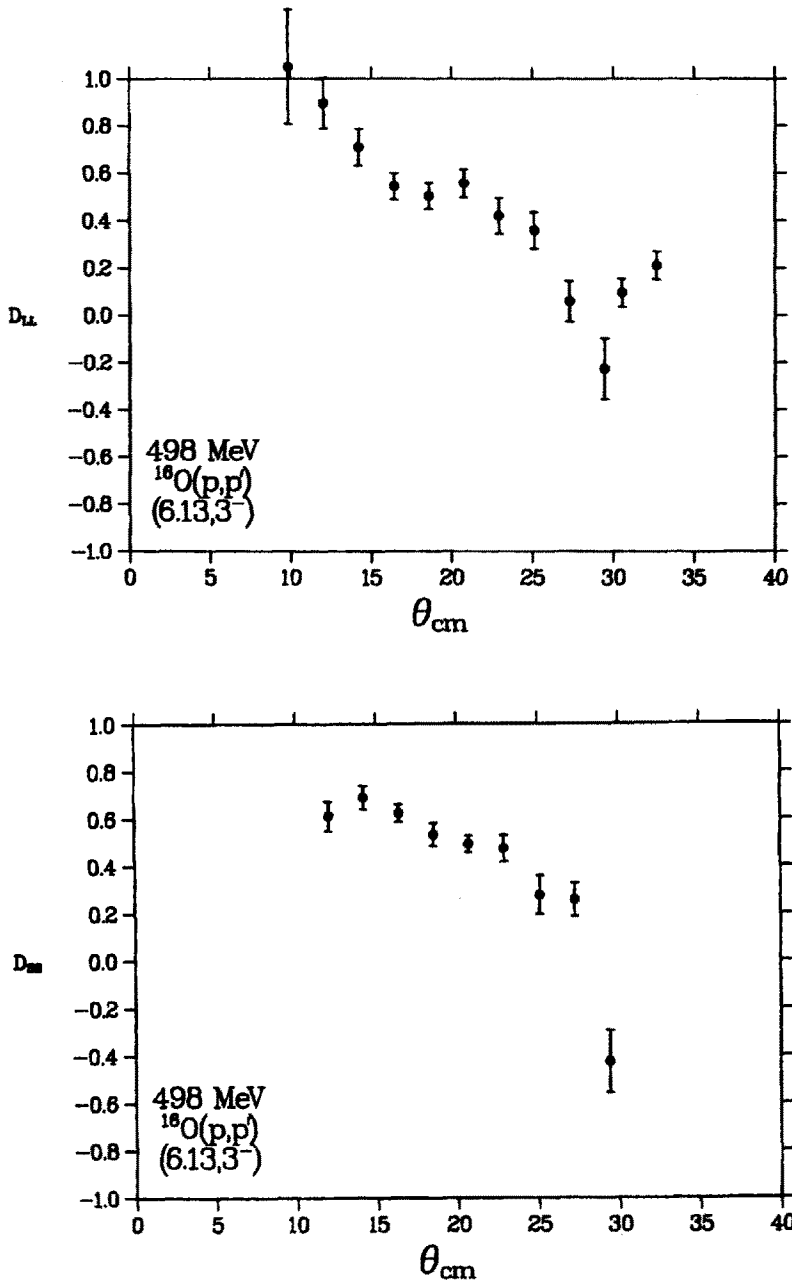


Figure 6. Preliminary values of  $D_{LL}$  (top) and  $D_{SS}$  (bottom) for the  $^{16}\text{O}(p,p')^{16}\text{O}(3^-, 6.13 \text{ MeV})$  reaction at 498 MeV (Ref. 9).

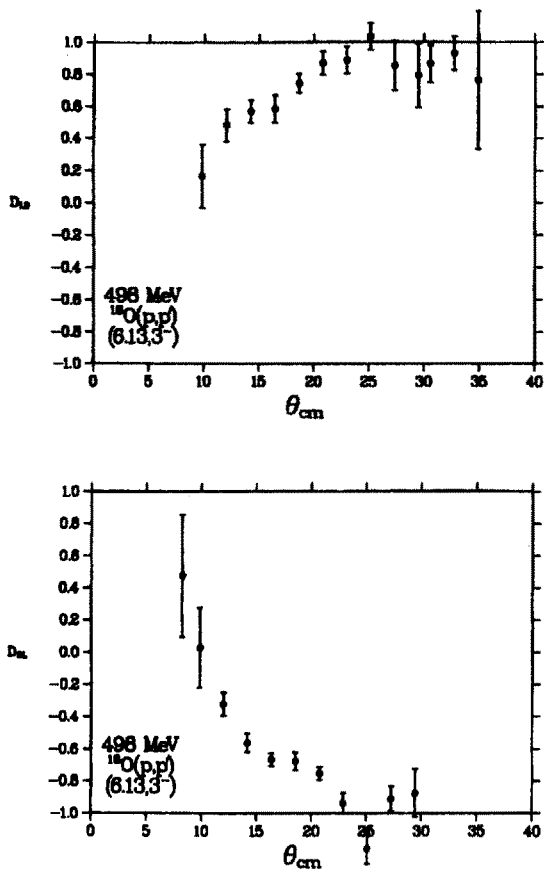


Figure 7. Preliminary values of  $D_{LS}$  (top) and  $D_{SL}$  (bottom) for the  $^{16}\text{O}(p,p')^{16}\text{O}(3^-, 6.13 \text{ MeV})$  reaction at 498 MeV (Ref. 9).

the nucleon-nucleon interaction.<sup>12</sup> These terms are labelled as  $|C_0|^2$ ,  $|C_1|^2$ , etc. in the figure; the notation for these amplitudes is that of Ref. 11. Presuming the nuclear structure is known, the measurement of these parameters is thus a direct measure of the effective nucleon-nucleon (NN) interaction inside nuclei, term by term. Note that the theoretical curves in Fig. 8 give quite a good account of the data; no serious problems are evident, for example, in the DWIA prediction calculated with the Love-Franey interaction (dashed curve).

It is somewhat surprising that no theoretical difficulties are encountered here, at least within the accuracy of the present

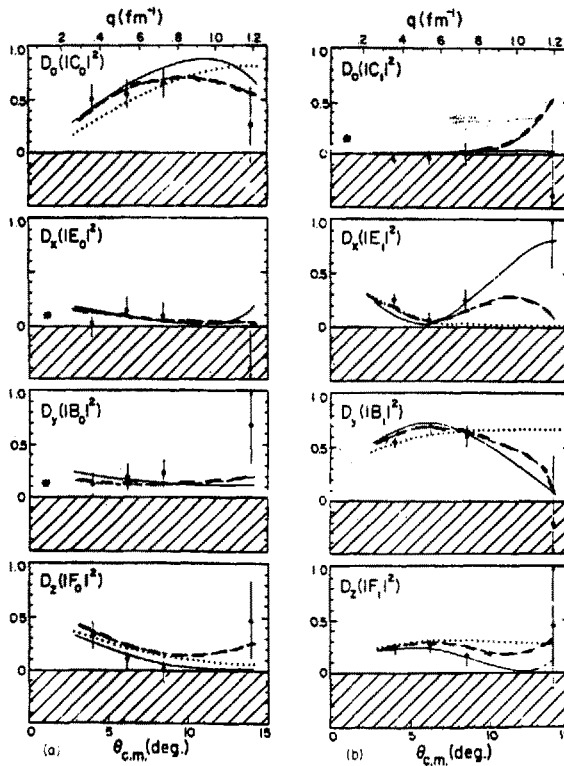


Figure 8. Spin observables for the  $^{12}\text{C}(p,p')^{12}\text{C}$  reaction at 500 MeV to the 12.71 MeV,  $1^+$ ,  $T=0$  state (left) and the 15.11 MeV,  $1^+$ ,  $T=1$  state (right). The observables plotted,  $D_O$ ,  $D_x$ ,  $D_y$ , and  $D_z$ , are combinations of the  $D_{ij}$  parameters described in the text; the shaded region is unphysical for these observables. Each is sensitive to the particular term in the NN interaction appearing in parentheses. The dotted curve is a plane wave impulse approximation calculation; the solid and dashed curves are Glauber Model and Love-Franey calculations, respectively (Ref. 11).

data, since similar data for elastic scattering at 500 MeV provided the first dramatic evidence that a non-relativistic impulse approximation was not satisfactory.<sup>13</sup> Considerable effort in the past few years has been expended on formulating a relativistic impulse approximation description of intermediate energy elastic scattering based primarily on the Dirac equation; indeed, this is one of the prime subjects of this meeting. Only now are the first preliminary

results of the relativistic calculations for inelastic scattering becoming available; the method has been formulated by J. Shepard, E. Rost, and J. McNeil.<sup>14</sup> The treatment has a number of interesting features, which should prove useful even if the specific relativistic effects turn out to be not so important. It introduces nuclear currents in a straightforward manner in the direct amplitude, and so provides a basis for easy comparison of proton, electron, and pion scattering. These currents include standard convection currents  $\langle j \rangle$  as well as "composite" currents  $\langle \sigma \cdot j \rangle$  and  $\langle \sigma x j \rangle$ . Some of these currents do not contribute to electron or pion scattering; they can be uniquely probed with protons. These currents appear also in non-relativistic DWIA treatments, but they enter only via non-localities and exchange effects. Whether they are equally large in relativistic and non-relativistic treatments remains to be seen. One of the interesting questions to be asked at this time is whether there is any evidence that these currents can be observed at all. Is there a new and confirming signature of relativity in the inelastic data?

It is certainly much too early to answer these questions, first because there are very few inelastic  $D_{ij}$  data and secondly because the relativistic calculations are very preliminary. The calculations have been made with non-relativistic nuclear wave functions and do not yet include exchange contributions (which should however be much smaller than exchange contributions in the non-relativistic treatments). In comparison with the 500 MeV data of McClelland et al.<sup>11</sup> for  $^{12}\text{C}$ , the relativistic predictions are very similar to the Love-Franey predictions and in good agreement with the data, except for  $D_{NN}$  and  $D_{SS}$  for the  $T=0$  state. For these two observables, the relativistic predictions agree well only when the convection current term is omitted. We now have new data at 500 MeV for the  $5^-$  state at 9.7 MeV in  $^{28}\text{Si}$ , as well as the  $6^-$   $T=0$  and  $T=1$  stretched states at 11.57 and 14.35 MeV. The differences between the relativistic and non-relativistic calculations of the  $D_{ij}$  for these states are also rather small, and the few preliminary data points cannot distinguish between them. However, there is a significant disagreement between both predictions and the preliminary  $A_y$  data for the  $5^-$  state.

When the standard collective model for strong natural parity transitions is treated relativistically, the effects of relativity appear at first sight to be dramatic. Sherif et al. have just obtained the first results of such a macroscopic relativistic

treatment in which the distorted waves are solutions of the Dirac equation with complex scalar and vector potentials, and the transition operator is obtained by deforming these potentials.<sup>15</sup> The nuclear collective states are treated non-relativistically. The method has been applied to 497 MeV data<sup>10</sup> for the  $3^-$  state in  $^{40}\text{Ca}$  as shown by the solid curve in Fig. 9; the agreement is excellent.

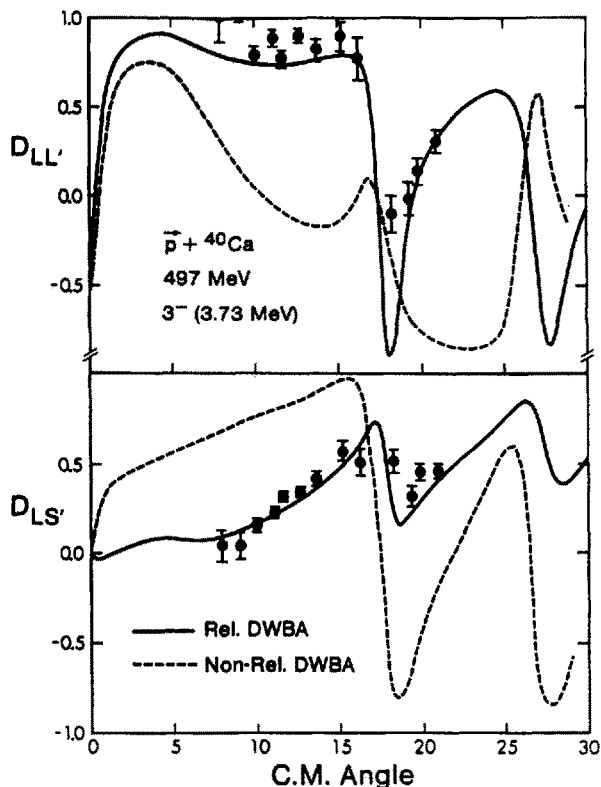


Figure 9. Macroscopic model calculations of spin rotation parameters for the  $^{40}\text{Ca}(p,p')^{40}\text{Ca}(3^-, 3.73 \text{ MeV})$  reaction at 497 MeV (Ref. 10). The two curves correspond to calculations with a relativistic and non-relativistic formalism (Ref. 15).

The dashed lines show the results of a standard non-relativistic macroscopic model calculation, and the results are much worse. Both calculations rely on phenomenological fits to the elastic scattering, and the non-relativistic fit is said<sup>15</sup> to be somewhat

worse than the relativistic fit to the elastic scattering. It may be that much of the difference between the solid and dashed curves in Fig. 9 can be attributed to this. Given the small differences between relativistic and non-relativistic results at the same incident energy obtained in the microscopic model by Shepard et al. as discussed above, the present macroscopic results should be viewed with some caution.

The first measurements of the  $D_{ij}$  parameters for inelastic scattering at the Indiana cyclotron have recently been reported by C. Olmer et al.<sup>16</sup> These data were taken at 200 MeV for the  $1^+$ ,  $T=0$  state in  $^{12}\text{C}$  at 12.71 MeV, and three stretched  $4^-$  states in  $^{16}\text{O}$ . The statistical accuracy of these data is very good, so that they provide a stringent test of both relativistic and non-relativistic calculations. Preliminary results are shown in Figs. 10-13. The quantities  $D_0$  and  $D_1$  plotted in Fig. 10 and 11 are again combinations of the  $D_{ij}$  parameters which are revealed in the relativistic treatment to be particularly sensitive to convection currents and composite currents, respectively. The results shown in Fig. 10 indicate that the relativistic calculation (dot-dashed and dotted curves) is much more sensitive to the convection current than the non-relativistic calculation is. The latter, however, provides a better fit to the data. The  $\sigma D_1$  data in Fig. 11 are explained about equally well by relativistic and non-relativistic treatments with composite currents included. It is the  $\langle \sigma \cdot j \rangle$  contributions rather than the  $\langle \sigma x j \rangle$  term which is important here, and both non-relativistic and relativistic calculations are very sensitive to it. (The relativistic calculation without this term is not shown.) Data and calculations for the individual  $D_{ij}$  for the 12.71 state are displayed in Fig. 12. In addition to the relativistic calculation (labelled Shepard-Rost), DWIA calculations with three different NN interactions are illustrated. No one of these curves provides a good fit to all the data shown; the relativistic calculation does about as well as the others. Given the preliminary nature of these calculations, this should surely be counted as a success. It is interesting that most of the differences between the non-relativistic predictions with the Love-Franey interaction and those with the free Paris interaction can be attributed to the different strengths of the imaginary tensor components in the two interactions. As an example of the results for  $^{16}\text{O}$ , the data and calculations for the  $4^-$ ,  $T=0$  state

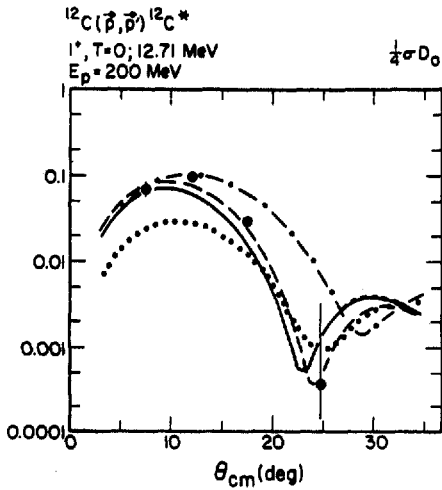


Figure 10. Preliminary values of the parameter  $\sigma D_0/4$ , where  $D_0 = 1 + D_{SS} + D_{LL} + D_{NN}$ . These data were taken at 200 MeV for the 12.71 MeV state in the  $^{12}\text{C}(p, p')^{12}\text{C}^*$  reaction. Calculations using the Love-Franey interaction are shown with (solid) and without (dash) the convection current contribution. Relativistic impulse approximation calculations are also shown with (dot) and without (dash-dot) this contribution (Ref. 16).

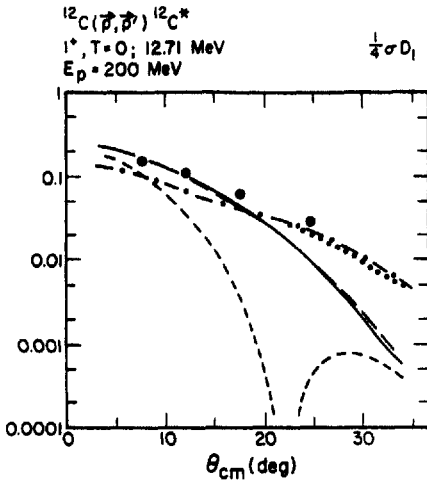


Figure 11. Preliminary values of the parameter  $\sigma D_1/4$ , where  $D_1 = 1 - D_{SS} + D_{LL} - D_{NN}$ , for the  $^{12}\text{C}(p, p')^{12}\text{C}(1^+, 12.71 \text{ MeV})$  reaction at 200 MeV. Calculations using the Love-Franey interaction are shown with (solid) and without (short dash) the composite current contribution. The dash-dot curve is the relativistic impulse approximation curve with the composite current included (Ref. 16).

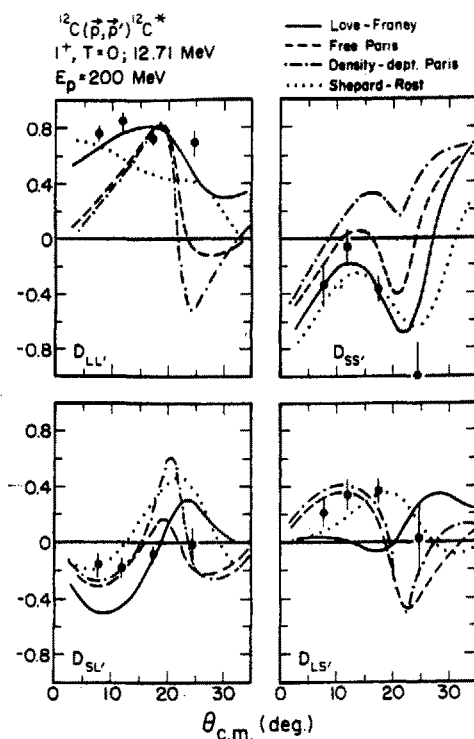


Figure 12. Preliminary values of spin rotation parameters  $D_{ij}$  measured at 200 MeV for the  $^{12}\text{C}(p, p')^{12}\text{C}(1^+, 12.71 \text{ MeV})$  reaction. The first three curves are theoretical predictions based on a non-relativistic DWIA formalism with three different NN interactions; the last curve (Shepard-Rost) is calculated using a Dirac approach (Ref. 16).

at 18.98 MeV are shown in Fig. 13. The relativistic predictions provide a good account of the data, failing mostly at the largest angles where the missing exchange effects are likely to be most important.

Finally, I want to comment briefly on a subject dear to my heart and also to the hearts of at least a few members of the audience, spin excitations. At LAMPF we have been exploring the M1 region and the continuum above it with measurements of  $D_{NN}$  at 319 MeV.<sup>17</sup> Our initial data for  $^{90}\text{Zr}$  were consistent with the assignment of M1 to a bump seen at an excitation energy of 9 MeV in cross section measurements at Orsay. These data also showed

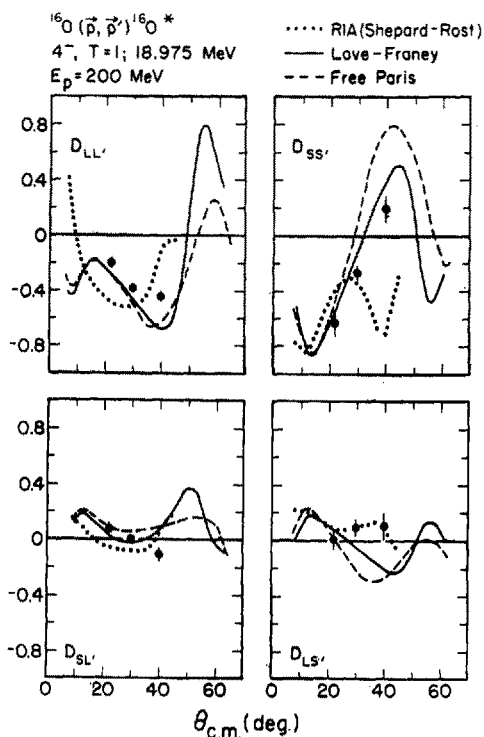


Figure 13. Preliminary values of spin rotation parameters  $D_{ij}$  and calculations as in Fig. 12 for the  $^{16}\text{O}(p, p')^{16}\text{O}$  ( $4^-$ , 18.98 MeV) reaction (Ref. 16).

a surprisingly large spin excitation strength in the continuum up to at least 25 MeV. A calculation (Fig. 14) by Esbensen and Bertsch in an infinite slab model can explain these data without any free parameters and without quenching.<sup>18</sup> The data have fairly large errors and the theoretical model is somewhat rough, so there is still room for possible quenching by, for example, the delta resonance. But the data and the calculation seem to suggest that all the "missing" M1 strength might be found in the region around the M1 state itself. The calculation of Esbensen and Bertsch predicts that the spin excitation cross section becomes much weaker above about 30 MeV excitation. Our more recent data, quite preliminary, shows that the spin-flip probability is rising up to 40 MeV excitation, and that the spin excitation cross section is roughly constant from 20 to 40 MeV excitation. In other words, our

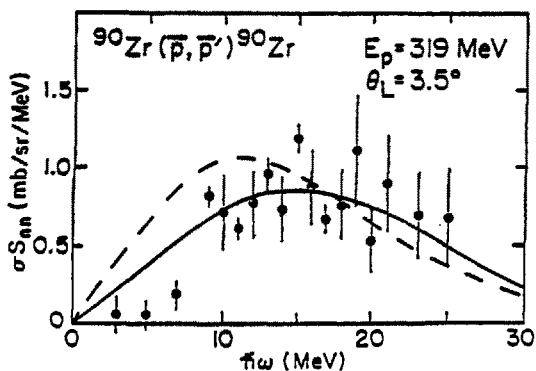


Figure 14. Comparison of the data of Ref. 17 at  $3.5^\circ$  with the theoretical calculations of Esbensen and Bertsch (Ref. 18). The curves shown are calculations with an infinite slab model of the nucleus with (solid) and without (dashed) RPA correlations.

data for  $^{90}\text{Zr}(p,p')$  seem similar to the data for the  $^{90}\text{Zr}(p,n)$  reaction. A detailed calculation, such as that currently underway by Osterfeld et al. at Jülich, and a multipole decomposition of the data are necessary to determine whether the  $(p,p')$  continuum near the M1 resonance is indeed hiding the missing strength.

We now have data for  $^{58}\text{Ni}$ , which appears quite similar to the data for  $^{90}\text{Zr}$ , and we also have data for  $^{51}\text{V}$ . The  $^{51}\text{V}$  data are particularly interesting because the spin-flip cross section spectrum shows a definite peak at the same excitation energy as the proposed M1 resonance seen in the cross section spectrum at Orsay.<sup>19</sup> These data, coupled with the observation of a strong peak at  $0^\circ$  in a cross section spectrum at LAMPF, strongly suggest that the resonance is indeed M1. Yet no definite M1 strength at all has been seen in this region in electron scattering data at Darmstadt.<sup>20</sup> The most likely explanation is that the broad M1 resonance in  $^{51}\text{V}$  is simply lost in the strong background of the electron spectrum.

These studies of spin excitations are only beginning; many nuclei need to be studied over a wide range of angles and energies in order to determine the spin excitation spectrum as reliably as the natural parity giant resonance spectrum is now known. This is clearly a fruitful area of research that will continue for a number of years. The application of relativistic methods to intermediate energy inelastic scattering is also in its very early stages. Much

theoretical work remains and appropriate experiments must be carried out to find all the new features that relativity promises.

#### Acknowledgements

The work described here in which I have participated requires the collaboration of a large number of scientists. Kevin Jones, John McGill, and Sirish Nanda have all made particularly important contributions. I am very grateful also to my colleagues who have sent me preliminary data and permitted me to discuss their work here; these include J. Kelly, D. Lopiano, C. Olmer, H. Sherif, and J. Shepard.

This work was supported in part by the National Science Foundation.

#### References

1. K. Jones et al., preprint, 1985.
2. F. Osterfeld et al., Nucl. Phys. A318, 45 (1979).
3. C. Djalali et al., Nucl. Phys. A380, 42 (1982);  
S. Kailas et al., Phys. Rev. C29, 2075 (1984).
4. A. Nakada, Y. Torizuka and Y. Horikawa, Phys. Rev. Lett. 27, 745 (1971).
5. K. Jones, private communication.
6. J. Kelly et al., preprint, 1985.
7. J. Kelly, Proc. Cretan Conference on Current Problems in Nuclear Physics, 1985, to be published.
8. J. McClelland et al., preprint, 1984.
9. D. Lopiano et al., private communication.
10. B. Aas et al., Phys. Rev. C26, 1770 (1982).
11. J. McClelland et al., Phys. Rev. Lett. 52, 98 (1984).
12. J. M. Moss, Phys. Rev. C26, 727 (1982);  
F. Bleszynski et al., Phys. Rev. C26, 2063 (1982).
13. A. Rahbar et al., Phys. Rev. Lett. 47, 1811 (1981);  
G. W. Hoffmann et al., Phys. Rev. Lett. 47, 1436 (1981).
14. J. Shepard, E. Rost, and J. McNeil, preprint, 1985.
15. H. S. Sherif, E. D. Cooper and R. I. Sawafta, preprint, 1985.
16. C. Olmer et al., Proceedings International Symposium on Nucleon and Anti-Nucleon Nucleus Scattering, Telluride, Colorado, 1985, to be published.
17. S. Nanda et al., Phys. Rev. Lett. 51, 1526 (1983).
18. H. Esbensen and G. Bertsch, Ann. Phys. 157, 255 (1984).
19. C. Djalali et al., Nucl. Phys. A388, 1 (1982).
20. D. Bender et al., Nucl Phys. A398, 408 (1983).